## Free3D: 3D Human Motion Emerges from Single-View 2D Supervision

# Sheng Liu Nanjing University

### Yuanzhi Liang TeleAI

## Sidan Du Nanjing University

anderliu@smail.nju.edu.cn

liangyzh18@outlook.com

coff128@nju.edu.cn

#### **Abstract**

Recent 3D human motion generation models demonstrate remarkable reconstruction accuracy yet struggle to generalize beyond training distributions. This limitation arises partly from the use of precise 3D supervision, which encourages models to fit fixed coordinate patterns instead of learning the essential 3D structure and motion–semantic cues required for robust generalization. To overcome this limitation, we propose Free3D, a framework that synthesizes realistic 3D motions without any 3D motion annotations. Free3D introduces a Motion-Lifting Residual Quantized VAE (ML-RQ) that maps 2D motion sequences into 3D-consistent latent spaces, and a suite of 3D-free regularization objectives enforcing view consistency, orientation coherence, and physical plausibility. Trained entirely on 2D motion data, Free3D generates diverse, temporally coherent, and semantically aligned 3D motions, achieving performance comparable to or even surpassing fully 3Dsupervised counterparts. These results suggest that relaxing explicit 3D supervision encourages stronger structural reasoning and generalization, offering a scalable and dataefficient paradigm for 3D motion generation.

#### 1. Introduction

Recent advances in 3D human motion generation [10, 35, 39] have led to models that achieve high numerical precision, reproducing training motions with very low reconstruction error and strong frame-level fidelity. However, despite these impressive scores, current systems often generalize poorly beyond their training distribution. They reproduce in-domain motions with excellent fidelity but struggle with unseen actions, new subjects, or compositional variations. The generated sequences, while visually coherent, tend to be overly constrained and exhibit limited diversity for the same textual or contextual input. For example, masked-token models like MoMask [10] often yield highly similar or even nearly identical samples under repeated generation [26]. This discrepancy naturally raises a question: does higher reconstruction accuracy truly indi-

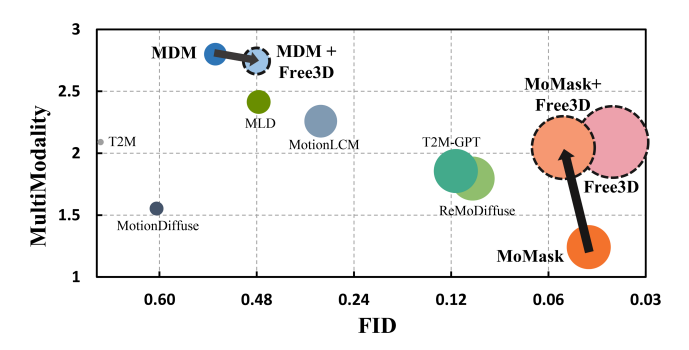


Figure 1. MultiModality-FID comparisons of different methods on HumanML3D dataset. 3D-supervised methods, such as MDM [31], tend to achieve low FID but relatively high MultiModality, whereas MoMask [10] exhibits the opposite trend. Free3D, trained solely with single-view 2D supervision, relaxes the constraints of precise 3D signals. This encourages the model to learn true motion structure and semantic patterns, enabling it to achieve both high MultiModality and low FID simultaneously. The point size of each method represents its Quality–Multimodality Score (QM), which jointly reflects FID and MultiModality through an integrated measure detailed in the experimental section.

cate better motion understanding, or does it instead reveal a limitation of the prevailing learning paradigm?

Most existing approaches [5, 10, 31, 38, 39] learn textdriven 3D motion by directly mapping textual inputs to 3D motion annotations. 3D motion data provide precise joint coordinates, but they are deterministic, expensive to collect, and typically limited in variety and coverage. Under such supervision, the learning objective is dominated by exact coordinate matching. In this setting, models can achieve strong benchmark performance by fitting datasetspecific motion patterns, without necessarily forming robust abstractions of motion structure or semantics. Recent analvses [19, 22] of VO-based motion generators have shown that representing motion via discrete tokens, coupled with reconstruction-oriented metrics, tends to reduce generation diversity and align models closely with the training distribution as in Fig. 1. At the same time, several works [21, 28] point out that reliance on curated 3D motion capture restricts motion diversity at the data level, simply because large-scale, richly varied 3D annotations are difficult and expensive to obtain. These findings suggest that full dependence on explicit 3D supervision may bias models toward reproducing precise coordinate patterns, limiting their ability to capture compositional structure, variability, and semantic richness in human motion.

This perspective motivates us to reconsider not only model architecture, but also the form of supervision used to learn 3D motion. Instead of further tightening the 3D supervision signal, we ask whether a more flexible target space could encourage models to infer structure rather than memorize coordinates. In this work, we explore learning 3D motion from 2D cues, using 2D motion as the only supervision signal. 2D motion sequences, readily extracted from images and videos, are significantly more diverse and abundant than 3D motion capture data. More importantly, the inherent ambiguity of 2D projection makes the training signal less over-determined: the model cannot simply copy exact 3D coordinates and is instead encouraged to reason about depth, body configuration, temporal coherence, and physical plausibility in order to explain the observed 2D motions. In this way, 2D supervision is not only easier to obtain, but also acts as a regularizing constraint that promotes structural reasoning and generalization.

To realize this idea, we propose 3D-Free Motion Generation (Free3D), a framework that synthesizes coherent and physically plausible 3D motions without using any 3D motion annotations during training. The design has three key components. First, a Free3D motion representation decomposes each motion into a global trajectory and relative limb vectors in both 2D and 3D, establishing a structured correspondence between projected and lifted motions. Second, a Motion Lifting Residual Quantized VAE (ML-RQ) encodes 2D motion sequences into a latent space, applies residual vector quantization, and decodes them into 3D motion sequences. This architecture allows the model to learn 3D-consistent latent codes purely from 2D supervision, without ever seeing ground-truth 3D poses. Third, a set of 3D-free regularization objectives—including viewconsistent projection losses, view-invariant priors via random rotations, orientation regularization, and feature-level consistency—enforces geometric stability, temporal coherence, and semantic alignment of the generated motion under diverse virtual viewpoints.

Extensive experiments show that Free3D, trained solely on 2D motion data, produces natural, diverse, and physically consistent 3D sequences, while maintaining strong alignment with textual descriptions. The framework attains performance competitive with, and in some cases surpassing, 3D-supervised baselines across standard benchmarks. These results challenge the conventional assumption that precise 3D annotations are indispensable for high-quality 3D motion generation, and support the view that carefully

relaxed supervision can lead to stronger structural reasoning and better generalization.

Contributions of this work can be summarized as follows:

- 1. We provide an analysis and empirical evidence suggesting that direct, fully precise 3D supervision can constrain generalization by encouraging coordinate-level fitting rather than structural understanding.
- 2. We introduce Free3D, a 3D-free motion generation framework that learns 3D motions from 2D cues through a Free3D representation, a Motion Lifting RQ-VAE, and physically motivated regularization.
- 3. We demonstrate that 2D-only supervision can yield competitive or superior 3D motion generation performance, revealing an alternative path toward scalable and generalizable 3D motion synthesis.

#### 2. Related Work

**Text-Driven Motion Generation.** Generating 3D human motion from textual descriptions has become an important research direction, aiming to synthesize semantically consistent and temporally coherent motions from language inputs [3, 5, 8–10, 15, 20, 24, 31, 35, 39, 40]. Existing approaches can be broadly categorized into diffusion-based and VAE-based methods. Diffusion models [14, 29, 30] generate motions by progressively denoising a latent sequence under a controlled diffusion process. MDM [31] first proposed predicting samples instead of noise, enabling geometric constraints during training. ReMoDiffuse [39] adds a retrieval mechanism to refine denoising, while MotionDiffuse [40], MotionLCM [5], and Fg-t2m++ [35] improve semantic alignment and temporal smoothness through enhanced latent diffusion strategies. VAE-based frameworks such as T2M [8] model the probabilistic relationship between text and motion sequences via temporal VAEs [23]. MotionGPT [15] and T2M-GPT [38] combine VAE-based latent motion representations with GPT-like architectures [1, 16] to achieve strong semantic consistency. MoMask [10] further introduces hierarchical quantization to represent motion as multi-level discrete codes [18]. Despite their success, all these methods rely heavily on 3D motion annotations, limiting their scalability in real-world settings where accurate 3D labels are scarce. This motivates exploration into frameworks that can reduce or even remove 3D supervision while maintaining high-quality, semantically accurate motion generation.

**Weakly-Supervised Motion Estimation.** Beyond motion generation, 3D human motion estimation seeks to recover 3D structure from 2D observations. To reduce dependence on dense 3D annotations, weakly supervised methods leverage unpaired 2D–3D data or train solely on abundant

2D inputs. Typical approaches learn compact 3D priors or low-dimensional bases from partial supervision to regularize reconstruction [4, 6, 11, 12, 17, 32, 34, 37]. Other works further minimize 3D reliance by enforcing geometric consistency or ambiguity-aware constraints directly from 2D cues, such as adversarial consistency [2], ambiguity mitigation [36], probabilistic flow modeling [33], and occlusionrobust extensions for multi-person cases [13]. Despite these advances, text-driven 3D motion generation under singleview 2D supervision remains highly challenging, as it requires both geometric reasoning and robust 2D motion priors. Building on these insights, our work introduces a 3D-Free framework that integrates the Free3D motion representation, Motion Lifting RQ-VAE, and 3D-Free regularization to achieve high-quality motion generation without any 3D labels.

#### 3. Preliminary: MoMask

MoMask [10] is a text-conditioned 3D human motion generation model that relies on 3D motion labels for supervised learning. The framework comprises three key components: an RVQ-VAE for motion representation learning, a Masked Transformer for capturing temporal dependencies, and a Residual Transformer for refining motion sequences.

**RVQ-VAE.** The RVQ-VAE encodes input motion sequences into latent embeddings  $z_{1:t}$  and applies multi-level residual vector quantization with L codebooks  $\{\mathcal{C}^l\}_{l=1}^L$ . At each level l, the quantizer refines the residuals left by the previous level, and the final quantized representation is obtained by summing all residual code vectors:

$$Q(z) = \sum_{l=1}^{L} q^{l}, \quad q^{l} = \arg\min_{c_{k}^{l} \in \mathcal{C}^{l}} \|r^{l} - c_{k}^{l}\|^{2}$$
 (1)

where  $r^1=z$  and  $r^l=r^{l-1}-q^{l-1}$ . The model is optimized using a reconstruction objective combined with a codebook commitment loss:

$$\mathcal{L}_{rvq} = \|m^{3D} - \hat{m}^{3D}\|_2 + \alpha \cdot \mathcal{L}_{commit}$$
 (2)

where  $\hat{m}^{3D}$  denotes the reconstructed 3D motion.

Masked and Residual Transformers. The Masked Transformer captures coarse spatiotemporal structures from the first-layer tokens under text conditioning, while the Residual Transformer refines finer motion details in subsequent layers. Text features are extracted with CLIP [27] and projected into embeddings  $e_{text}$  via a fully connected layer. The Masked Transformer  $p_{\theta}$  is trained to minimize the negative log-likelihood of the first-layer tokens:

$$\mathcal{L}_{NLL} = \sum_{\substack{x_{mask}^{(1)} \\ x_{mask}^{(2)}}} -\log p_{\theta}(x^{(1)}|x_{mask}^{(1)}, e_{text})$$
 (3)

The Residual Transformer  $p_{\phi}$  optimizes the remaining layers similarly:

$$\mathcal{L}_{res} = \sum_{l=2}^{L} -\log p_{\phi}(x^{(l)}|x^{(1:l-1)}, e_{text}, l)$$
 (4)

where  $x^{(l)}$  denote the tokens of l-th layer.

**Inference.** The inference process adopts classifier-free guidance and proceeds in three stages. First, the Masked Transformer iteratively generates the base-layer tokens through masked sampling and refinement. Next, the Residual Transformer progressively predicts tokens for the remaining quantization layers. Finally, all quantized tokens are decoded by the RVQ-VAE decoder to reconstruct the complete 3D motion sequence.

#### 4. 3D-Free Motion Generation

Our goal is to train a 3D motion generation model without relying on any 3D motion annotations, enabling the framework to scale to scenarios where 3D data are unavailable or impossible to capture. As illustrated in Fig. 2, our approach consists of three key components: the Free3D motion representation (Sec. 4.1) that facilitates the construction of 3D-free regularization, a generation architecture (Sec. 4.2) that produces coherent and physically plausible 3D motion sequences, and the 3D-free regularization (Sec. 4.3) that enforces physical and temporal consistency without explicit 3D supervision.

#### 4.1. Free3D Motion Representation

Let  $v^{3D}$  represents a set of 3D limb vectors defined as:

$$v^{3D} = \{j^{parent(n)} - j^{child(n)}\}_{n=1}^{K}$$
 (5)

where K is the number of limbs.  $j^{parent(n)}$  and  $j^{child(n)}$  denote the parent and child joints of n-th limb, respectively. We decompose a 3D motion sequence  $m_{1:T}^{3D}$  into a global trajectory sequence  $\tau_{1:T}$  and a relative motion sequence  $v_{1:T}^{3D}$ :

$$m_{1 \cdot T}^{3D} = \{ \tau_{1 \cdot T}, v_{1 \cdot T}^{3D} \} \tag{6}$$

This decomposition separates global translation from local articulation, which allows the model to explicitly capture the intrinsic correspondence between 3D relative motion and 2D relative motion. Since our goal is to train the model without any 3D motion supervision, we instead leverage 2D motion data as supervisory signals. Similarly to the representation of 3D relative motion, a 2D relative motion can be represented as a sequence  $v_{1:T}^{2D}$ , where each  $v_{1:T}^{2D}$  is a set of 2D limb vectors describing the relative configuration of body parts. Therefore, the 2D motion can be represented as:

$$m_{1:T}^{2D} = \{\tau_{1:T}, v_{1:T}^{2D}\}\tag{7}$$

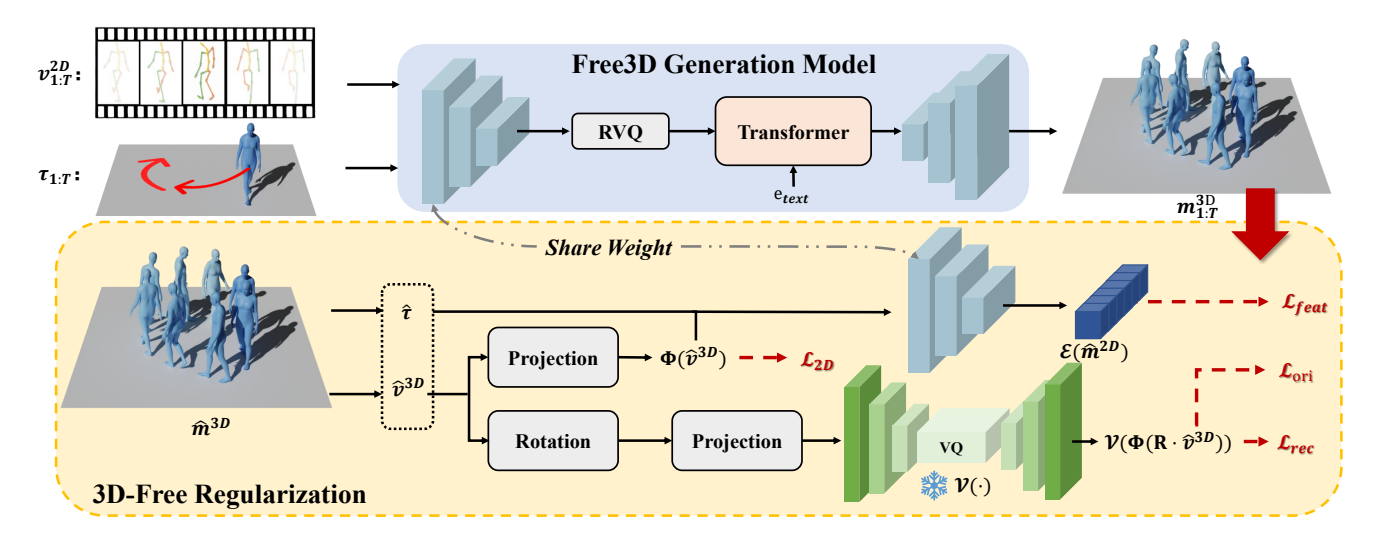


Figure 2. The pipeline of our method. Free3D can generate consistent and physically plausible 3D motions without relying on any 3D annotations, using only single-view 2D motion supervision. The decoupled global trajectory and 2D motion sequences are first encoded into a latent space via the Motion Lifting Residual Quantized VAE (ML-RQ) and then decoded into 3D motion. A set of 3D-free regularization objectives—including view-consistent projection losses, view-invariant priors through random rotations, orientation regularization, and feature-level consistency—is applied to enforce geometric stability, temporal coherence, and semantic alignment of the generated motions. Similar to MoMask [10], motion generation is performed in the quantized latent space produced by the encoder.

#### 4.2. 3D-Free Generation Architecture

Although our generative framework is built upon MoMask [10] as the baseline, MoMask [10] relies on 3D motion labels to supervise the training of its RVQ-VAE. To achieve 3D motion generation without any 3D motion annotations, we propose the Motion Lifting RQ-VAE (ML-RQ), which is designed to bridge the gap between 2D and 3D motion representations by leveraging only 2D motion information. The key intuition is that the temporal dynamics and limb topology inherent in 2D motions already contain rich spatial cues that can be effectively lifted into 3D space. Specifically, ML-RQ encodes the 2D motion input into a latent space and applies a residual quantizer  $Q(\cdot)$  to discretize the latent representation. The quantized features are then passed through a decoder to generate the corresponding 3D motion sequence, enabling unsupervised lifting from 2D motions to 3D motions.

$$m_{1:T}^{3D} = \mathcal{D}(\mathcal{Q}(\mathcal{E}(m_{1:T}^{2D}))) \tag{8}$$

where  $\mathcal{E}(\cdot)$  and  $\mathcal{D}(\cdot)$  denote the encoder and decoder, respectively. This design allows the model to learn 3D-consistent motion representations from 3D-Free Regularization (see Sec. 4.3 for the regularization strategy):

$$\mathcal{L}_{MLRQ} = \mathcal{L}_{req} + \beta \cdot \mathcal{L}_{commit} \tag{9}$$

where  $\mathcal{L}_{reg}$  is the term of 3D-Free regularization and  $\mathcal{L}_{commit}$  is the term of commitment loss.  $\beta$  is a weighting factor

#### 4.3. 3D-Free Regularization

**View-Consistent Prior Regularization.** To enhance the spatial coherence and physical plausibility of the 3D motions  $\hat{m}^{3D} = \{\hat{\tau}, \hat{v}^{3D}\}$  produced by ML-RQ, we introduce a View-Consistent Prior Regularization (VCPR). This regularization consists of two complementary components:

Firstly, we enforce the projected 2D motion of the generated 3D sequence to align with the corresponding 2D supervision:

$$\mathcal{L}_{2D} = \|\Phi(\hat{v}^{3D}) - v^{2D}\|_{2}^{2} + \|\hat{\tau} - \tau\|_{2}^{2} \tag{10}$$

where  $\Phi(\cdot)$  is a weak-perspective projection operator, which approximates the camera projection without requiring explicit intrinsic parameters.

Second, to further improve view-invariant consistency under the single-view 2D supervision setting, we assume that a physically plausible 3D motion should yield 2D projections that remain consistent with the natural 2D motion distribution under arbitrary viewpoints. To leverage this assumption without access to multi-view or 3D annotations, we first train a VQ-VAE on real 2D motions to learn the underlying 2D distribution. During ML-RQ training, the VQ-VAE is frozen, and its reconstruction error is used as a regularization term on randomly rotated projections, encouraging the generated 3D motions to remain plausible across multiple viewpoints:

$$\mathcal{L}_{rec} = \|\mathcal{V}(\Phi(R \cdot \hat{v}^{3D})) - \Phi(R \cdot \hat{v}^{3D})\|_{2}^{2}$$
 (11)

where R denotes a random rotation and  $V(\cdot)$  represents the frozen VQ-VAE pretrained on 2D motions.

Orientation Regularization. To further enhance the physical plausibility of the generated 3D motions, we introduce Orientation Regularization. We observe that in realistic human motions, the global body orientation and the foot directions almost always share the same forward trend. Although they may not be perfectly aligned, their directions remain consistently coherent. In other words, the projection of the foot direction vector onto the body orientation vector should be non-negative. Based on this observation, we impose an orientation consistency constraint during training to encourage the model to produce spatially natural and physically plausible motions:

$$\mathcal{L}_{ori} = \max(0, -\hat{v}_{foot} \cdot \hat{v}_{ori}) \tag{12}$$

where  $\hat{v}_{ori}$  denotes the body orientation vector, which can be computed as the normalized cross product of the left and right hip vectors:

$$\hat{v}_{ori} = \frac{\hat{v}_{rhip} \times \hat{v}_{lhip}}{\|\hat{v}_{rhip} \times \hat{v}_{lhip}\|_2}$$
(13)

**Feature Consistency Regularization.** To ensure the latent representation remains semantically consistent with 2D supervision, we introduce Feature Consistency Regularization (FCR). While direct supervision constrains the output motion at the data level, discrepancies may still arise in the latent space. To mitigate this, we feed the projected motion into the encoder  $\mathcal{E}(\cdot)$  for encouraging feature-level alignment and representation consistency:

$$\mathcal{L}_{feat} = \|\mathcal{E}(\hat{m}^{2D}) - \mathcal{E}(m^{2D})\|_2^2 \tag{14}$$

where  $\hat{m}^{2D}=\{\hat{\tau},\Phi(\hat{v}^{3D})\}$  denotes the projected 2D motion derived from the generated 3D sequence.

**Overall Regularization.** The overall 3D-Free regularization term is defined as the weighted combination of all the aforementioned regularization objectives:

$$\mathcal{L}_{req} = \mathcal{L}_{2D} + \lambda_1 \cdot \mathcal{L}_{rec} + \lambda_2 \cdot \mathcal{L}_{ori} + \lambda_3 \cdot \mathcal{L}_{feat} \quad (15)$$

where each  $\lambda$  controls the relative contribution of the corresponding loss term.

#### 5. Experiments

**Datasets.** We evaluate our approach on two major motion-language benchmarks: HumanML3D [8] and KIT-ML [25]. The **HumanML3D** dataset contains 14,616 motion samples from the AMASS [21] and HumanAct12 [7] datasets, each paired with three unique text descriptions, totaling 44,970 descriptions. The **KIT-ML** [23] dataset integrates data from multiple motion capture sources into a unified format, with 3,911 motion sequences and 6,278 text descriptions, providing a smaller benchmark for evaluation.

**Evaluation Metrics.** We adopt several standard metrics to evaluate motion quality, diversity, and text—motion alignment. FID measures the distance between generated and real motion feature distributions, where lower values indicate higher realism. R-Precision assesses semantic alignment by checking whether the correct text ranks within the top-k retrieved (k=1,2,3). MMDist is the average Euclidean distance between motion and text features, reflecting cross-modal consistency. Diversity quantifies variability across different text inputs, while MultiModality (MModality) measures variance among motions generated from the same text, capturing conditional diversity. To jointly evaluate overall generation quality and diversity under identical conditions, we introduce the Quality—MModeality Score (QM), defined as:

QM Score = 
$$\sqrt{\frac{\text{MModality}}{\text{FID}}}$$
 (16)

A higher QM indicates a better balance between motion quality and diversity, providing a more holistic evaluation of generative performance.

#### **5.1. Implementation Details.**

**Model Details.** Following MoMask [10], our ML-RQ module employs a 6-layer residual vector quantizer, where each codebook has a dimension of 512 and contains 512 code entries. Both the encoder and decoder consist of three residual 1D convolutional layers. For the VQ-VAE that learns the 2D motion distribution, we use a single codebook while keeping the other configurations identical. The architectures of the Transformers also follow those in MoMask [10] for fair comparison.

**Training Details.** In our experiments, Free3D is trained in three stages: ML-RQ, Masked Transformer, and Residual Transformer. For ML-RQ training, we set  $\lambda_1 = \lambda_2 = \lambda_3 = 1$  and  $\beta = 2$ . The model is optimized using the Adam optimizer with a batch size of 256. We first pretrain ML-RQ with a learning rate of 0.0002, followed by fine-tuning with a smaller learning rate of 0.0002. For the Masked Transformer and Residual Transformer, we use a learning rate of 0.0002 and the same batch size of 256. All experiments are conducted on a single RTX 3090 GPU.

#### 5.2. Quantitative Results.

We report quantitative results on two benchmark datasets. Unlike prior methods [3, 5, 8, 10, 31, 35, 38–40] that require 3D motion data, Free3D is trained only with single-view 2D supervision, highlighting its ability to perform competitively without 3D annotations.

**Comparison on HumanML3D.** Since Free3D is the first 3D motion generation framework trained solely under

Table 1. Quantitative evaluation on the HumanML3D test set.  $\pm$  indicates a 95% confidence interval. 'S.V.' denotes using single-view 2D motion for supervision. '3D Finetune' indicates that Free3D is first trained with 2D supervision to extract features, which are then fused into a 3D-supervised model and fine-tuned.

Supervision	Methods	Top 1	R Precision Top 2	Top 3	FID↓	MMDist↓	$Diversity \rightarrow$	MModality↑	QM Score↑
	Real	0.511 <sup>±.003</sup>	$0.703^{\pm.003}$	$0.797^{\pm.002}$	$0.002^{\pm.000}$	$2.974^{\pm.008}$	$9.503^{\pm.065}$	-	-
	T2M [8] MDM [31] MLD [3] MotionDiffuse [40]	$0.320^{\pm .005} \ 0.481^{\pm .003}$	$0.498^{\pm .004} \ 0.673^{\pm .003}$	$0.611^{\pm .007} \\ 0.772^{\pm .002}$	$0.544^{\pm.044}$ $0.473^{\pm.013}$	$5.566^{\pm.027}$	$9.188^{\pm.002}$ $9.559^{\pm.086}$ $9.724^{\pm.082}$ $9.410^{\pm.049}$	$2.090^{\pm.083}$ $2.799^{\pm.072}$ $2.413^{\pm.079}$ $1.553^{\pm.042}$	1.400 2.268 2.259 1.570
3D Motion	ReMoDiffuse [39] T2M-GPT [38] MotionLCM [5] MoMask [10] Fg-T2M++ [35]	$0.510^{\pm.005}$ $0.491^{\pm.003}$ $0.502^{\pm.003}$ $0.521^{\pm.002}$	$0.698^{\pm.006}$ $0.680^{\pm.003}$ $0.698^{\pm.002}$ $0.713^{\pm.002}$	$0.795^{\pm .004}$ $0.775^{\pm .002}$ $0.798^{\pm .002}$ $\boldsymbol{0.807}^{\pm .002}$	$0.103^{\pm.004}$ $0.116^{\pm.004}$ $0.304^{\pm.012}$ $0.045^{\pm.002}$	$2.974^{\pm.016}$ $3.118^{\pm.011}$ $3.012^{\pm.007}$	9.018 <sup>±.075</sup> 9.761 <sup>±.081</sup> 9.607 <sup>±.066</sup>	$1.795^{\pm .043}$ $1.856^{\pm .011}$ $2.259^{\pm .092}$ $1.241^{\pm .040}$ $2.625^{\pm .084}$	4.175 4.000 2.726 5.251 5.431
S.V. 2D Motion	Free3D (3D Finetune) Free3D (MDM-Based) Free3D (MoMask-Based)	$0.435^{\pm.005}$	$0.618^{\pm.006}$	$0.746^{\pm.006}$	$0.480^{\pm.038}$	$3.010^{\pm.008}$ $3.650^{\pm.011}$ $3.155^{\pm.009}$	9.489 <sup>±.084</sup> 9.513 <sup>±.083</sup> 9.486 <sup>±.048</sup>	$2.090^{\pm.072}$ $2.743^{\pm.080}$ $2.046^{\pm.068}$	<b>7.416</b> 2.391 6.155

Table 2. Quantitative evaluation on the KIT-ML test set.  $\pm$  indicates a 95% confidence interval. 'S.V.' denotes using single-view 2D motion for supervision. '3D Finetune' indicates that Free3D is first trained with 2D supervision to extract features, which are then fused into a 3D-supervised model and fine-tuned.

Supervision	Methods	Top 1	R Precision 1 Top 2	Top 3	FID↓	MMDist↓	$Diversity \rightarrow$	MModality↑	QM Score↑
	Real	$0.424^{\pm.005}$	$0.649^{\pm.006}$	$0.779^{\pm.006}$	$0.031^{\pm.004}$	$2.788^{\pm.012}$	$11.08^{\pm.097}$	-	-
	T2M [8]	$0.370^{\pm.005}$	$0.569^{\pm.007}$	$0.693^{\pm.007}$	$2.770^{\pm.109}$	$3.401^{\pm.008}$	10.91 <sup>±.119</sup>	1.482 <sup>±.065</sup>	0.731
	MDM [31]	$0.164^{\pm.004}$	$0.291^{\pm .004}$	$0.396^{\pm.004}$	$0.497^{\pm.021}$	$9.191^{\pm.022}$	$10.85^{\pm.109}$	$1.907^{\pm .214}$	1.956
	MLD [3]	$0.390^{\pm.008}$	$0.609^{\pm.008}$	$0.734^{\pm.007}$	$0.404^{\pm.027}$	$3.204^{\pm.027}$	$10.80^{\pm.117}$	$2.192^{\pm.071}$	2.329
2D Madian	MotionDiffuse [40]	$0.417^{\pm.004}$	$0.621^{\pm .004}$	$0.739^{\pm.004}$	$1.954^{\pm.062}$	$2.958^{\pm.005}$	$11.10^{\pm.143}$	$0.730^{\pm.013}$	0.611
3D Motion	ReMoDiffuse [39]	$0.427^{\pm.014}$	$0.641^{\pm.004}$	$0.765^{\pm.055}$	$0.155^{\pm.006}$	$2.814^{\pm.012}$	$10.80^{\pm.105}$	$1.239^{\pm.028}$	2.827
	T2M-GPT [38]	$0.416^{\pm .006}$	$0.627^{\pm.006}$	$0.745^{\pm.006}$	$0.514^{\pm.029}$	$3.007^{\pm.023}$	$10.92^{\pm.108}$	$1.570^{\pm.039}$	1.748
	MoMask [10]	$0.433^{\pm.007}$	$0.656^{\pm.005}$	$0.781^{\pm.005}$	$0.204^{\pm.011}$	$2.779^{\pm.022}$	-	$1.131^{\pm.043}$	2.355
S.V. 2D Motion	Free3D (3D Finetune)	0.458 <sup>±.006</sup>	0.680 <sup>±.005</sup>	<b>0.794</b> <sup>±.005</sup>	<b>0.153</b> <sup>±.013</sup>	2.635 <sup>±.020</sup>	$10.79^{\pm.114}$	$2.171^{\pm.078}$	3.767
	Free3D (MDM-Based)	$0.436^{\pm.004}$	$0.644^{\pm.004}$	$0.757^{\pm.005}$	$0.294^{\pm.019}$	$2.979^{\pm.024}$	$10.49^{\pm.112}$	$2.698^{\pm.084}$	3.029
	Free3D (MoMask-Based)	$0.413^{\pm.008}$	$0.634^{\pm.007}$	$0.763^{\pm.007}$	$0.248^{\pm.016}$	$2.993^{\pm.025}$	$11.25^{\pm.109}$	$2.481^{\pm.074}$	3.163

single-view 2D supervision, we compare it against recent state-of-the-art (SOTA) methods that rely on full 3D supervision on the HumanML3D dataset. As shown in Tab. 1, Free3D, trained with only single-view 2D motion supervision, achieves a FID score of 0.054, demonstrating performance comparable to current state-of-the-art methods. In terms of R-Precision, Free3D also achieves results close to the best-performing models. Notably, Free3D achieves the highest QM score, indicating that when jointly considering FID and MultiModality, Free3D exhibits the strongest overall generation performance. Furthermore, when the features learned under 2D supervision are fused and fine-tuned with those from the 3D-supervised MoMask [10], the FID further improves to 0.038, setting a new SOTA, while achieving the best Diversity score and a substantial gain in MultiModality. These results highlight that 2D-derived representations contain complementary structural priors that can enrich 3D motion understanding. In line with our motivation, this suggests that reducing dependence on precise 3D ground truth not only alleviates overfitting but also encourages models to reason about motion structure more abstractly, thereby enhancing generalization to unseen scenarios.

Comparison on KIT-ML. As shown in Tab. 2, we further evaluate Free3D on KIT-ML. The results demonstrate that Free3D, trained solely with 2D motion supervision, maintains performance comparable to current state-of-theart methods across key metrics such as FID and R-Precision. Importantly, it attains the top QM score, highlighting its superior ability to balance motion realism with generative diversity under identical textual conditions. When the 2D-learned features are fused and fine-tuned with those from 3D-supervised models, the performance further improves,

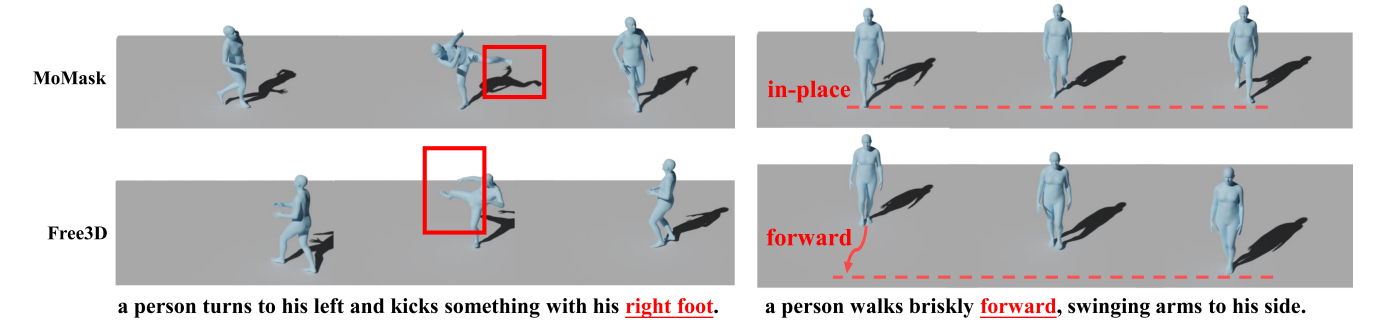
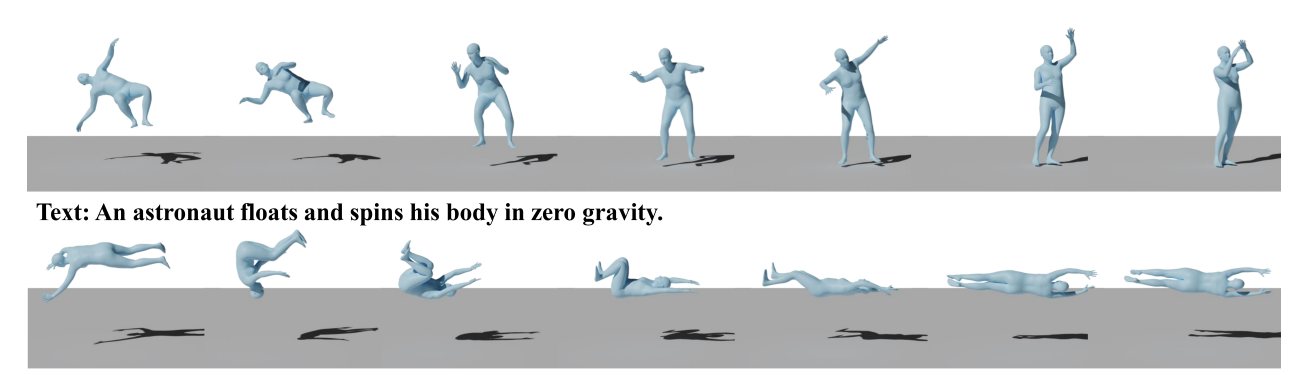


Figure 3. Qualitative comparison on HumanML3D dataset. Compared with MoMask [10], our method demonstrates better generalization and a more accurate understanding of textual semantics, producing motions that more closely align with the given text descriptions.



Text: A man turns his body and kicks his legs while swimming underwater.

Figure 4. Qualitative Results on In-the-Wild Motions. Free3D is capable of learning from and generating motions extracted from inthe-wild 2D videos. We selected several actions that cannot be physically performed or captured with 3D motion sensors under existing conditions, extracted their 2D motion sequences, and used them for supervision. Free3D successfully generates high-quality 3D motions for these challenging scenarios, despite the absence of 3D annotations.

achieving state-of-the-art results. This confirms that representations learned from 2D supervision capture rich structural and semantic cues that complement 3D-based features. Consistent with our analysis in the introduction, these findings suggest that precise 3D supervision, while beneficial for numerical accuracy, may overconstrain model learning and limit generalization. In contrast, the underdetermined nature of 2D supervision encourages models to infer structural relationships rather than memorize coordinates, leading to more robust and diverse motion generation.

#### 5.3. Qualitative Results.

Qualitative comparisons with SOTA 3D-supervised methods are shown in Fig. 3. Compared to MoMask [10], Free3D generates motions more aligned with textual semantics, demonstrating that 2D supervision improves generalization. Since Free3D requires no 3D annotations, it can be directly applied to in-the-wild video data, learning motions difficult or impossible to capture in 3D. As shown in Fig. 4, it synthesizes realistic microgravity and underwater motions. Additional results are provided in the supplementary material, highlighting Free3D's potential for scalable

and diverse 3D motion generation.

#### 5.4. Ablation Studies.

Ablation Study on 3D-Free Regularization. Free3D aims to achieve 3D label-free training through the introduction of 3D-Free regularization, making the ablation and in-depth analysis of each regularization term essential. The results in Tab. 3 verify the necessity of all three components. Among them, the 2D distribution reconstruction plays the most critical role in improving generation quality. By reconstructing 2D motions of different views, it effectively constrains the multi-view consistency of the generated results and helps the model learn a more accurate 3D spatial structure from purely 2D cues. In addition, both feature consistency regularization and orientation regularization further enhance motion generation quality. The orientation regularization encourages the model to learn consistent and physically plausible body orientations across frames, thereby improving the temporal coherence and realism of generated motions. Meanwhile, feature consistency regularization acts as a latent-space constraint that regularizes the distribution of encoded features, stabilizing the repre-

Table 3. Ablation Study on 3D-Free Regularization.

Config.		Precision Top 2		FID	MMDist	Diversity	MModality
Real	0.511	0.703	0.797	0.002	2.974	9.503	-
w.o. $\mathcal{L}_{rec}$	0.368	0.551	0.678	2.588	3.912	8.449	2.127
w.o. $\mathcal{L}_{ori}$	0.465	0.656	0.756	0.124	3.282	9.299	2.225
w.o. $\mathcal{L}_{feat}$	0.501	0.686	0.780	0.088	3.125	9.450	2.086
Ours	0.487	0.681	0.780	0.054	3.155	9.486	2.046

Table 4. Ablation Study on 2D Motion Distribution Learning and parameter sharing in FCR.

Config.	R Precision Top 1 Top 2 Top 3			FID	MMDist	Diversity	MModality
Real	0.511	0.703	0.797	0.002	2.974	9.503	-
with VAE	0.467	0.657	0.753	0.121	3.247	9.218	2.168
with AE	0.450	0.648	0.753	0.258	3.295	9.198	2.040
w.o. sharing	0.477	0.660	0.759	0.120	3.281	9.230	2.147
Ours	0.487	0.681	0.780	0.054	3.155	9.486	2.046

Table 5. Comparison of ML-RQ reconstructions on various representations. 'w,j.c' denotes using joint coordinates.

Config.	MPJPE R Precision				FID	MMDist	Diversity	
	(mm)	Top 1	Top 2	Top 3	FID	MIMIDIST	Diversity	
Real	0	0.511	0.703	0.797	0.002	2.974	9.503	
w.j.c	106.9	0.390	0.574	0.688	3.902	3.843	8.303	
Ours	56.4	0.487	0.681	0.780	0.054	3.155	9.486	

sentation learning process and helping the model better disentangle motion semantics from spatial geometry. Collectively, these components enable Free3D to learn 3D-aware motion representations purely from 2D supervision.

## Ablation Study on 2D Motion Distribution Learning.

To learn the prior distribution of 2D motions, Free3D adopts a VQ-VAE architecture for modeling. To verify its necessity, we compare the performance of using VAE and plain AE for distribution learning. As shown in Tab. 4, the results indicate that the performance of VAE is significantly weaker than that of VQ-VAE, while AE performs even worse. This performance gap arises because VQ-VAE, through vector quantization, introduces a discrete representation in the latent space, enabling the model to learn more stable and semantically consistent motion patterns, thus better capturing the structural characteristics of 2D motion distributions. In contrast, the VAE relies on continuous latent variables that often lead to blurred distribution boundaries, while the AE lacks explicit distribution modeling capability and can only perform point-to-point reconstruction, failing to capture the global statistical regularities of motion data. Therefore, VQ-VAE demonstrates clear superiority in learning a highquality prior of 2D motion distributions, serving as a crucial component that supports ours 3D-free training paradigm.

**Ablation Study on Parameter Sharing in FCR.** During FCR, Free3D utilizes the encoder shared with ML-RQ for feature encoding. This design choice is motivated by the fact that ML-RQ is trained on a large set of real 2D motions, enabling the encoder to learn stable and robust feature representations. By reusing this pre-trained encoder, Free3D effectively maps input 2D motions into the latent space while preserving essential spatial and temporal structures, facilitating more accurate 3D motion generation. The results in Tab. 4 further validate the effectiveness of this parameter-sharing strategy. When encoder parameters are not shared, the model's FID score decreases significantly, indicating a drop in generation quality. This demonstrates that the shared encoder provides more consistent and reliable features, allowing the model to better capture the spatial geometry and dynamic variations of motions.

Ablation Study on Free3D Representation. In our experiments, Free3D adopts a limb vector-based representation. This choice is motivated by the fact that limb vectors naturally encode the relative structural relationships of the human skeleton, making it easier for the model to capture geometric constraints and temporal coherence of motions. Additionally, this representation reduces the influence of scale differences between joints on feature learning, thereby improving the stability and accuracy of 3D motion generation. In Tab. 5, we also present the reconstruction quality of ML-RQ when using different representations, including an experiment with joint coordinates directly as the representation. However, this approach ignores the internal skeletal topology, making the model more dependent on absolute positions and more sensitive to noise and scale variations. As a result, the reconstruction quality drops significantly, leading to a substantial performance gap compared to Free3D using limb vectors.

#### 6. Conclusion

We have presented Free3D, a novel 3D-free motion generation framework that learns to synthesize highly realistic 3D human motions purely from 2D supervision. Unlike existing 3D-supervised methods that optimize for coordinatelevel accuracy, Free3D actively promotes structural understanding through a flexible 2D-3D representation, a Motion Lifting Residual Quantized VAE, and geometry-aware regularization objectives. Our results convincingly demonstrate that high-quality and semantically aligned 3D motion can emerge without relying on accurate 3D ground truth, achieving performance on par with or beyond 3Dsupervised baselines. This finding challenges the longstanding assumption that dense 3D annotations are indispensable for effective motion learning. We believe Free3D opens a promising direction toward scalable, annotationefficient, and generalizable 3D motion generation.

#### References

- [1] Tom Brown, Benjamin Mann, Nick Ryder, Melanie Subbiah, Jared D Kaplan, Prafulla Dhariwal, Arvind Neelakantan, Pranav Shyam, Girish Sastry, Amanda Askell, et al. Language models are few-shot learners. Advances in neural information processing systems, 33:1877–1901, 2020.
- [2] Ching-Hang Chen, Ambrish Tyagi, Amit Agrawal, Dylan Drover, Rohith Mv, Stefan Stojanov, and James M Rehg. Unsupervised 3d pose estimation with geometric selfsupervision. In *Proceedings of the IEEE/CVF Conference* on Computer Vision and Pattern Recognition, pages 5714– 5724, 2019. 3
- [3] Xin Chen, Biao Jiang, Wen Liu, Zilong Huang, Bin Fu, Tao Chen, and Gang Yu. Executing your commands via motion diffusion in latent space. In *Proceedings of the IEEE/CVF Conference on Computer Vision and Pattern Recognition*, pages 18000–18010, 2023. 2, 5, 6
- [4] Zhihua Chen, Xiaoli Liu, Bing Sheng, and Ping Li. Garnet: Graph attention residual networks based on adversarial learning for 3d human pose estimation. In Advances in Computer Graphics: 37th Computer Graphics International Conference, CGI 2020, Geneva, Switzerland, October 20–23, 2020, Proceedings, pages 276–287. Springer, 2020. 3
- [5] Wenxun Dai, Ling-Hao Chen, Jingbo Wang, Jinpeng Liu, Bo Dai, and Yansong Tang. Motionlcm: Real-time controllable motion generation via latent consistency model. In *European Conference on Computer Vision*, pages 390–408. Springer, 2024. 1, 2, 5, 6
- [6] Dylan Drover, Rohith MV, Ching-Hang Chen, Amit Agrawal, Ambrish Tyagi, and Cong Phuoc Huynh. Can 3d pose be learned from 2d projections alone? In *Proceedings* of the European Conference on Computer Vision (ECCV) Workshops, pages 0–0, 2018. 3
- [7] Chuan Guo, Xinxin Zuo, Sen Wang, Shihao Zou, Qingyao Sun, Annan Deng, Minglun Gong, and Li Cheng. Action2motion: Conditioned generation of 3d human motions. In *Proceedings of the 28th ACM International Conference on Multimedia*, pages 2021–2029, 2020. 5
- [8] Chuan Guo, Shihao Zou, Xinxin Zuo, Sen Wang, Wei Ji, Xingyu Li, and Li Cheng. Generating diverse and natural 3d human motions from text. In *Proceedings of the IEEE/CVF Conference on Computer Vision and Pattern Recognition*, pages 5152–5161, 2022. 2, 5, 6
- [9] Chuan Guo, Xinxin Zuo, Sen Wang, and Li Cheng. Tm2t: Stochastic and tokenized modeling for the reciprocal generation of 3d human motions and texts. In *European Conference* on Computer Vision, pages 580–597. Springer, 2022.
- [10] Chuan Guo, Yuxuan Mu, Muhammad Gohar Javed, Sen Wang, and Li Cheng. Momask: Generative masked modeling of 3d human motions. In *Proceedings of the IEEE/CVF* Conference on Computer Vision and Pattern Recognition, pages 1900–1910, 2024. 1, 2, 3, 4, 5, 6, 7
- [11] Julian Habekost, Takaaki Shiratori, Yuting Ye, Taku Komura, M Shi, K Aberman, A Aristidou, D Lischinski, D Cohen-Or, B Chen, et al. Learning 3d global human motion estimation from unpaired, disjoint datasets. In *BMVC*, 2020. 3

- [12] Ikhsanul Habibie, Weipeng Xu, Dushyant Mehta, Gerard Pons-Moll, and Christian Theobalt. In the wild human pose estimation using explicit 2d features and intermediate 3d representations. In *Proceedings of the IEEE/CVF conference* on computer vision and pattern recognition, pages 10905– 10914, 2019. 3
- [13] Peter Hardy and Hansung Kim. Links" lifting independent keypoints"-partial pose lifting for occlusion handling with improved accuracy in 2d-3d human pose estimation. In *Proceedings of the IEEE/CVF Winter Conference on Applications of Computer Vision*, pages 3426–3435, 2024. 3
- [14] Jonathan Ho, Ajay Jain, and Pieter Abbeel. Denoising diffusion probabilistic models. *Advances in neural information processing systems*, 33:6840–6851, 2020. 2
- [15] Biao Jiang, Xin Chen, Wen Liu, Jingyi Yu, Gang Yu, and Tao Chen. Motiongpt: Human motion as a foreign language. Advances in Neural Information Processing Systems, 36:20067–20079, 2023. 2
- [16] Takeshi Kojima, Shixiang Shane Gu, Machel Reid, Yutaka Matsuo, and Yusuke Iwasawa. Large language models are zero-shot reasoners. Advances in neural information processing systems, 35:22199–22213, 2022. 2
- [17] Jogendra Nath Kundu, Siddharth Seth, Varun Jampani, Mugalodi Rakesh, R Venkatesh Babu, and Anirban Chakraborty. Self-supervised 3d human pose estimation via part guided novel image synthesis. In *Proceedings of the IEEE/CVF conference on computer vision and pattern recognition*, pages 6152–6162, 2020. 3
- [18] Doyup Lee, Chiheon Kim, Saehoon Kim, Minsu Cho, and Wook-Shin Han. Autoregressive image generation using residual quantization. In *Proceedings of the IEEE/CVF con*ference on computer vision and pattern recognition, pages 11523–11532, 2022. 2
- [19] Weiyuan Li, Bin Dai, Ziyi Zhou, Qi Yao, and Baoyuan Wang. Controlling character motions without observable driving source. In Proceedings of the IEEE/CVF Winter Conference on Applications of Computer Vision, pages 6194– 6203, 2024. 1
- [20] Han Liang, Jiacheng Bao, Ruichi Zhang, Sihan Ren, Yuecheng Xu, Sibei Yang, Xin Chen, Jingyi Yu, and Lan Xu. Omg: Towards open-vocabulary motion generation via mixture of controllers. In *Proceedings of the IEEE/CVF Con*ference on Computer Vision and Pattern Recognition, pages 482–493, 2024. 2
- [21] Naureen Mahmood, Nima Ghorbani, Nikolaus F Troje, Gerard Pons-Moll, and Michael J Black. Amass: Archive of motion capture as surface shapes. In *Proceedings of the IEEE/CVF international conference on computer vision*, pages 5442–5451, 2019. 1, 5
- [22] Zichong Meng, Yiming Xie, Xiaogang Peng, Zeyu Han, and Huaizu Jiang. Rethinking diffusion for text-driven human motion generation: Redundant representations, evaluation, and masked autoregression. In *Proceedings of the Computer* Vision and Pattern Recognition Conference, pages 27859– 27871, 2025. 1
- [23] Mathis Petrovich, Michael J Black, and Gül Varol. Actionconditioned 3d human motion synthesis with transformer

- vae. In Proceedings of the IEEE/CVF International Conference on Computer Vision, pages 10985–10995, 2021. 2, 5
- [24] Mathis Petrovich, Michael J Black, and Gül Varol. Temos: Generating diverse human motions from textual descriptions. In European Conference on Computer Vision, pages 480–497. Springer, 2022. 2
- [25] Matthias Plappert, Christian Mandery, and Tamim Asfour. The kit motion-language dataset. *Big data*, 4(4):236–252, 2016. 5
- [26] Zheng Qin, Yabing Wang, Minghui Yang, Sanping Zhou, Ming Yang, and Le Wang. Embracing aleatoric uncertainty: Generating diverse 3d human motion. arXiv preprint arXiv:2508.20604, 2025. 1
- [27] Alec Radford, Jong Wook Kim, Chris Hallacy, Aditya Ramesh, Gabriel Goh, Sandhini Agarwal, Girish Sastry, Amanda Askell, Pamela Mishkin, Jack Clark, et al. Learning transferable visual models from natural language supervision. In *International conference on machine learning*, pages 8748–8763. PMLR, 2021. 3
- [28] Zeping Ren, Shaoli Huang, and Xiu Li. Realistic human motion generation with cross-diffusion models. In *European Conference on Computer Vision*, pages 345–362. Springer, 2024.
- [29] Jiaming Song, Chenlin Meng, and Stefano Ermon. Denoising diffusion implicit models. arXiv preprint arXiv:2010.02502, 2020. 2
- [30] Yang Song, Prafulla Dhariwal, Mark Chen, and Ilya Sutskever. Consistency models. In Proceedings of the 40th International Conference on Machine Learning, pages 32211–32252, 2023. 2
- [31] Guy Tevet, Sigal Raab, Brian Gordon, Yoni Shafir, Daniel Cohen-or, and Amit Haim Bermano. Human motion diffusion model. In *The Eleventh International Conference on Learning Representations*, 2023. 1, 2, 5, 6
- [32] Bastian Wandt and Bodo Rosenhahn. Repnet: Weakly supervised training of an adversarial reprojection network for 3d human pose estimation. In *Proceedings of the IEEE/CVF conference on computer vision and pattern recognition*, pages 7782–7791, 2019. 3
- [33] Bastian Wandt, James J Little, and Helge Rhodin. Elepose: Unsupervised 3d human pose estimation by predicting camera elevation and learning normalizing flows on 2d poses. In *Proceedings of the IEEE/CVF Conference on Computer Vision and Pattern Recognition*, pages 6635–6645, 2022. 3
- [34] Chaoyang Wang, Chen Kong, and Simon Lucey. Distill knowledge from nrsfm for weakly supervised 3d pose learning. In *Proceedings of the IEEE/CVF international conference on computer vision*, pages 743–752, 2019. 3
- [35] Yin Wang, Mu Li, Jiapeng Liu, Zhiying Leng, Frederick WB Li, Ziyao Zhang, and Xiaohui Liang. Fg-t2m++: Llms-augmented fine-grained text driven human motion generation. *International Journal of Computer Vision*, pages 1–17, 2025. 1, 2, 5, 6
- [36] Zhenbo Yu, Bingbing Ni, Jingwei Xu, Junjie Wang, Chenglong Zhao, and Wenjun Zhang. Towards alleviating the modeling ambiguity of unsupervised monocular 3d human pose

- estimation. In *Proceedings of the IEEE/CVF International Conference on Computer Vision*, pages 8651–8660, 2021. 3
- [37] Andrei Zanfir, Eduard Gabriel Bazavan, Hongyi Xu, William T Freeman, Rahul Sukthankar, and Cristian Sminchisescu. Weakly supervised 3d human pose and shape reconstruction with normalizing flows. In Computer Vision– ECCV 2020: 16th European Conference, Glasgow, UK, August 23–28, 2020, Proceedings, Part VI 16, pages 465–481. Springer, 2020. 3
- [38] Jianrong Zhang, Yangsong Zhang, Xiaodong Cun, Yong Zhang, Hongwei Zhao, Hongtao Lu, Xi Shen, and Ying Shan. Generating human motion from textual descriptions with discrete representations. In *Proceedings of the IEEE/CVF conference on computer vision and pattern recognition*, pages 14730–14740, 2023. 1, 2, 5, 6
- [39] Mingyuan Zhang, Xinying Guo, Liang Pan, Zhongang Cai, Fangzhou Hong, Huirong Li, Lei Yang, and Ziwei Liu. Remodiffuse: Retrieval-augmented motion diffusion model. In Proceedings of the IEEE/CVF International Conference on Computer Vision, pages 364–373, 2023. 1, 2, 6
- [40] Mingyuan Zhang, Zhongang Cai, Liang Pan, Fangzhou Hong, Xinying Guo, Lei Yang, and Ziwei Liu. Motiondiffuse: Text-driven human motion generation with diffusion model. *IEEE transactions on pattern analysis and machine intelligence*, 46(6):4115–4128, 2024. 2, 5, 6